



OPEN ACCESS

EDITED BY

Shaowei Zhang,
Institute of Deep-Sea Science and
Engineering (CAS), China

REVIEWED BY

Manuel Vargas-Yáñez,
Spanish Institute of Oceanography (IEO),
Spain
Bangyi Tao,
Ministry of Natural Resources, China
Wenwen Li,
Arizona State University, United States
Mingqiang Guo,
China University of Geosciences Wuhan,
China

*CORRESPONDENCE

Miaomiao Song

✉ mmsong@qlu.edu.cn

Shizhe Chen

✉ chensz@qlu.edu.cn

†These authors share first authorship

RECEIVED 30 December 2022

ACCEPTED 27 March 2023

PUBLISHED 28 April 2023

CITATION

Liu S, Song M, Chen S, Fu X, Zheng S,
Hu W, Gao S and Cheng K (2023) An
intelligent modeling framework to
optimize the spatial layout of ocean
moored buoy observing networks.
Front. Mar. Sci. 10:1134418.
doi: 10.3389/fmars.2023.1134418

COPYRIGHT

© 2023 Liu, Song, Chen, Fu, Zheng, Hu, Gao
and Cheng. This is an open-access article
distributed under the terms of the [Creative
Commons Attribution License \(CC BY\)](https://creativecommons.org/licenses/by/4.0/). The
use, distribution or reproduction in other
forums is permitted, provided the original
author(s) and the copyright owner(s) are
credited and that the original publication in
this journal is cited, in accordance with
accepted academic practice. No use,
distribution or reproduction is permitted
which does not comply with these terms.

An intelligent modeling framework to optimize the spatial layout of ocean moored buoy observing networks

Shixuan Liu^{1,2,3,4†}, Miaomiao Song^{1,3,4*†}, Shizhe Chen^{1,3,4*},
Xiao Fu^{1,3,4}, Shanshan Zheng^{1,3,4}, Wei Hu¹, Saiyu Gao¹
and Kaiyu Cheng¹

¹Institute of Oceanographic Instrumentation, Qilu University of Technology (Shandong Academy of Sciences), Qingdao, China, ²College of Engineering, Ocean University of China, Qingdao, China, ³National Marine Monitoring Equipment Engineering Technology Research Center, Qingdao, China, ⁴School of Ocean Technology Sciences, Qilu University of Technology (Shandong Academy of Sciences), Qingdao, China

This research is motivated by the practical requirements in the sustainable deployment of ocean moored buoy observing networks. Ocean moored buoys play an important role in the global marine environment monitoring. Ocean buoy station layout planning is a typical multiple-objective spatial optimization problem that aims to reduce the spatial correlation of buoy stations and improve their spatial monitoring efficiency. In this paper, we develop a multi-objective mathematical model for allocating ocean buoy stations (MOLMofOBS) based on Tobler's first law of geography. A spatial neighborhood model based on a Voronoi diagram is built to represent the spatial proximity of distributed buoy stations and delimit the effective monitoring region of every station. Then, a heuristic method based on a multiple-objective particles swarm optimization (MOPSO) algorithm is developed to calculate the MOLMofOBS via a dynamic inertia weight strategy. Meanwhile, a series of experiments is conducted to verify the efficiency of the proposed model and algorithms in solving single- and multiple-buoy station location problems. Finally, an interactive portal is developed in the Cyberinfrastructure environment to provide decision-making services for online real-time planning of the ocean buoy station locations. The work reported in this paper will provide spatial decision-making support for the sustainable development of ocean buoy observing networks.

KEYWORDS

multiple-objective location modeling, particles swarm optimization, Voronoi diagram, decision-support system, ocean moored buoy

1 Introduction

Marine monitoring is an important foundation and prerequisite for understanding, developing, and utilizing the ocean. As key marine monitoring equipment, ocean moored buoys can be equipped with various sensors according to the needs of various monitoring purposes, providing a reliable observation platform to collect and transmit real-time hydrological and meteorological data with the characteristics of being systematic, long-term, continuous, and stable on a daily basis. All over the world, several ocean buoy networks have been established for monitoring and forecasting ocean conditions and ocean–atmosphere interactions. In the Aegean Sea, the POSEIDON buoy network (Nittis et al., 2002; Nittis et al., 2006) consisting of 11 ocean buoys provides the opportunity to measure wind, atmospheric pressure, conductivity, ocean current speed, dissolved oxygen water temperature, and other properties. The triangle Trans-Ocean Buoy Network (TRITON) (Kashino et al., 2007; Hase et al., 2008) buoys were deployed in the western equatorial Pacific by Japan Agency for Marine–Earth Science and Technology (JAMSTEC) to observe El Niño/La Niña Southern Oscillation (ENSO), and the Tropical Atmospheric Ocean (TAO) (McPhaden et al., 1998), with more than 70 mooring buoys, were deployed by the National Oceanic and Atmospheric Administration (NOAA) of the United States. The Prediction and Research Moored Array in the Tropical Atlantic (PIRATA) (Bourles et al., 2008; Rouault et al., 2009) observation network consists of 18 mooring buoys and 3 island-based observation sites to observe climate and weather for prediction in the Tropical Atlantic. Argos (Tang et al., 2015) is another famous international program, which started in January 2000 and is devoted to deploying free-drifting buoys to collect and transmit temperature and salinity profile data in the upper 2000 meters of the global ocean. In the Argos buoy system, there are a total of about 16,000 buoys deployed around the world, of which about 3,900 are currently in operation. The ocean buoy network in China is strong and growing quickly, consisting of nearly 50 mooring buoys deployed by China Ministry of Natural Resources, 30 deployed by China Meteorological Bureau, and more than 30 others deployed by other institutes and departments (Wang et al., 2016).

Ocean moored buoy networks in several countries belong to different organizations in the fields of oceanography, meteorology, transportation, environment, fishery, scientific research, and industries. On one hand, different organizations make plans independently. On the other hand, there is actually a lack of effective methods to simulate and model the buoy spatial layout to achieve optimal configuration and allocation in the long term. These issues lead to insufficient integration of the existing buoy monitoring resources and limit the possibility of planning the scientific layout of future ocean monitoring activities. The rationality of the ocean buoys layout in an explicit marine space can be measured in terms of two aspects: 1) whether the density of buoy stations in the ocean monitoring network is appropriate, which significantly impacts the accuracy of the climate and weather prediction and the precision of marine science analysis such as globally meshing Argos data; and 2) whether the locations

of the buoy stations are sufficient and reasonable, which is directly related to the correctness of revealing the inherent variability of broad-scale and short-scale marine phenomena, such as water masses, ocean currents, and ocean fronts.

In view of the urgent needs for planning ocean moored buoy observing networks and addressing the key problems of buoy layout optimization, this paper carries out a spatial analysis of ocean buoy station locations to realize their location modeling for spatial optimization and to find efficient methods to calculate new potential positions for deploying additional ocean buoys. The work reported in this paper is of great significance to supporting decision-making for buoy layout planning as well as facilitating the construction of high-density and multi-parameter marine comprehensive observation networks.

This paper is organized as follows. Section 2 details spatial optimization problems and existing techniques by consulting the existing literature. This is followed by the realization of the spatial optimization modeling of ocean buoy stations, including conducting buoy station location modeling in Section 3, building the spatial neighborhood model of buoy sites, and designing an efficient multi-objective particle swarm optimization (PSO) algorithm for solving the location problem in Section 4. Then, a series of experiments is undertaken to demonstrate the efficiency and performance of the built spatial optimization model in Section 5, and an online application is established to provide planning services for ocean buoy station locations in Section 6. Finally, conclusions are provided in Section 7.

2 Related work

Optimizing the spatial layout of an ocean moored buoy observing network aims to maximize the spatial coverage of marine buoy monitoring stations by improving their scientific and rational deployment. It is a multidisciplinary problem involving spatial optimization, spatio-temporal analysis, intelligent computing, and other fields. The essence of this problem is to maximize or minimize one or more mathematical functions to solve the allocation scheme of public facilities resources, such as the locations of fire stations, hospitals, schools, and environmental monitoring stations, as well as reserve site selection (Church et al., 1996; Malcolma and Reville, 2005; Murray, 2010; Tong and Murray, 2012). Approaches for such location modeling focus on the P-median location-allocation model (Church and Wang, 2020; Zaferanieh et al., 2022), the maximum minimization model (Wang and Zhang, 2012), the maximum coverage location problem (MCLP) (Atta et al., 2021; Taiwo, 2021), and continuous model of coverage problem (CMCP) (Yang et al., 2020; Blanco and Gázquez, 2021). Based on the vertex weights and correction costs as independent uncertain variables (both side length and vertex weights are variable), Soltanpour et al. (2020) proposed a model of an uncertain inverse P-median location problem to deal with tail values at risk targets and proved that it is a nondeterminism Polynomial(NP) problem; meanwhile, a hybrid PSO algorithm was proposed to obtain the approximate optimal

solution of the proposed model. [Nguyen et al. \(2021\)](#) solved the connected P-median problem on fully multilayered graphs and developed an algorithm for solving the P-median problem based on the branch-and-bound principle. Arana-Jimenez et al ([Arana-Jiménez et al., 2020](#)). extended the fuzzy mathematics field of the maximum coverage location model, modeled from the fuzzy perspective, and generated appropriate Pareto solutions; a solution algorithm based on the augmented weighted Tchebycheff method was proposed, which could ensure the optimal Pareto solution. Casas-Ramirez et al ([Casas-Ramírez et al., 2020](#)). studied the bi-level maximum coverage localization problem and proposed a heuristic method based on a genetic algorithm with local search to obtain the lower bound of the optimal solution. Wang et al ([Wang et al., 2016](#); [Wang et al., 2020](#)). adopted the MCPL model and took the maximum area covered by the stations as the optimization objective to solve the precipitation station location problem and plan their optimal deployment. [Song et al. \(2021\)](#) set up a nonlinear continuous maximum coverage positioning model (CMCP-Ocean) to deploy a sustainable ocean buoy observation network and built a heuristic framework based on a PSO algorithm to solve the CMCP-Ocean model.

The ocean moored buoy location problem is regarded as an NP problem because the volume of potential solutions will be so large as to cause a combined explosion so that the problem is hardly solved within the time of polynomial complexity as the number of ocean buoys for deployment increases. Promising and practical heuristic algorithms, including PSO ([Shifa et al., 2011](#)), ant colony, simulated annealing, genetic, tabu search, greedy, and neural network algorithms have all been well applied to solve spatial optimization problems in fields such as regionalization ([Liu et al., 2015](#)), resource allocation and scheduling ([Chang and Wei, 2002](#)), and urban planning ([Feng and Liu, 2013](#)). Recently, hybrid heuristic methods have been highlighted to solve large instances of districting and regionalization problems ([Duque et al., 2012](#); [Kim et al., 2016](#)). ([Li et al., 2014](#)) constructed an extendable heuristic framework by integrating a semi-greedy algorithm and improved local search to generate p regions that are as compact as possible from n atomic polygons, defined as the p -compact-regions problem, which is a representative non-linear regionalization problem in urban economic modeling. ([Kim et al., 2016](#)) proposed a hybrid heuristic algorithm by combining the Automated Zoning Procedure and a center interchange method, improving the efficiency and the quality of solutions for large-size p -functional region problems. ([Kollat and Reed, 2007](#)) built an efficient framework for long-term groundwater monitoring planning using evolutionary multi-objective optimization techniques.

Among them, the PSO and multiple-objective PSO (MOPSO) algorithms show outstanding performance due to the organic adhesion and bidirectional influences of the local search phrase and the global search phrase by adjusting particles' position and speed while referring to the individual optimal solution and the global optimal solution in each iteration. Additionally, PSO-based algorithms have a strong advantage in solving the problem of multi-station site selection because the position and flight velocity dimensions of each particle only need to be expanded

horizontally as the number of stations to be calculated increases. The addition in particle dimensions will not enlarge the complexity of the optimization problem, nor the computational complexity, which has been verified in some research ([Shifa et al., 2011](#); [Masoomi et al., 2013](#); [Xie and Xu, 2017](#)). However, both traditional PSO and MOPSO have two major disadvantages: 1) the fixed or inappropriate inertia weight factor (ω) leads to the linear attenuation of particle velocity, which makes the flight behavior of particles tend to homoplasmy, resulting in local convergence that causes the search for optimal solutions to become entrapped in local areas from which it is unable to jump out; and 2) the particle search behavior is random and lacks diversity, which leads to the uneven distribution of particles in the feasible solution space and possible failure to reach the region where the best solution is located. These shortcomings become more obvious and difficult to solve for multi-objective optimization problems.

To address these issues, two kinds of strategies are carried out in relevant research. The first strategy type is to dynamically adjust the search step in the search stage to achieve the effect of refining the search granularity and increasing the diversity of particles. In this scope, strategies based on inertia weight (IW), which is an important parameter to balance the exploitation of individuals in local search and evolution of generations in global search, are created ([Chen et al., 2006](#); [Uma et al., 2012](#); [Chauhan et al., 2013](#); [Amoshahy et al., 2016](#)). For example, [Amoshahy et al. \(2016\)](#) proposed another more superior IW called the Flexible Exponential Inertia Weight (FEIW) strategy, which is also time-varying-based and has the ability to adapt with each optimization problem by selecting suitable parameters to make IW increase and decrease. Chen et al ([Li et al., 2014](#)). created a natural exponential IW strategy to dynamically vary IW according to the number of iterations to accelerate the decrease of inertia weight, which hastens convergence. The second strategy type comprises archival non-inferior solution maintenance and the global optimal solution selection strategy to provide the correct guidance for global leaders to local search in the evolution stage. In this aspect, exclusive and fuzzy Pareto dominance concepts ([AlvarezBenitez et al., 2005](#); [Köppen and Veenhuis, 2006](#)) are commonly adopted in multi-objective problems to select global optimal solutions, and marked effects with good convergence and widespread coverage are obtained. Meanwhile, the Pareto archive evolution strategy ([Knowles and Corne, 1999](#); [Zhao et al., 2012](#); [Knowles and Corne, 2014](#)) is employed to record and update non-dominated solutions, so as to provide a repository from which calculating the distribution density of non-inferior solutions, as well as selecting the global optimal and deleting redundancy solutions, can be carried out. In addition, the crowding distance sorting strategy ([Raquel and Naval, 2005](#); [Santana et al., 2009](#); [Feng et al., 2010](#)) has been proposed as a promising method to best approximate the true Pareto front by selecting the individual with the biggest crowding distance as the global optimum to make the swarm evolve to the sparse objective space, as well as by deleting the individual with the smallest crowding distance in the external Pareto archive to reduce the redundancy of non-dominant solutions.

3 Location modeling of ocean moored buoy station

3.1 Multi-objective location selection modeling of ocean moored buoy stations

The ocean moored buoy location problem can be abstracted as follows: in a given range of marine space, under the premise of not changing the existing buoy stations' positions, find suitable positions to deploy a number of ocean buoys with the aims of increasing the density of observation and avoiding duplicate monitoring and monitoring gaps. Furthermore, two objectives are required to be achieved for computation: the first objective is that the distribution of buoy stations should be as dispersive as possible to reduce the correlation of adjacent buoy stations, and the second objective is that the area of each buoy's effective monitoring region (EMR) should be as similar as possible to achieve a uniform layout of ocean buoy stations. Based on Tobler's first law of geography (Tobler, 1970; Klippel and Li, 2011) that near things are more related to each other, we take advantage of the Euclidean distances between the selected site and each site in its neighborhood to measure the first objective. All distances are expected to be as large as possible to match the goal. To address the second objective mentioned above, standard deviation is employed as the indicator to measure the uniformity of EMR. A smaller standard deviation of EMR areas would indicate a more uniform distribution. Therefore, the multi-objective location model of ocean buoy stations (MOLMofOBS) is formulated as follows:

$$\text{Maximize}(F_1) \tag{1}$$

$$\text{Minimize}(F_2) \tag{2}$$

where,

$$F_1 = \min(\{d_{i,j} | i = 1, \dots, n, P_j \in Nb(P_i)\}) \tag{3}$$

$$F_2 = \max(\{STD(\{S_{vi}, \{S_{vj}(j = 1, \dots, n) | v_j \text{ is the EMR of } P_i, \forall P_j \in Nb(P_i)\})\} | i = 1, \dots, n\}) \tag{4}$$

Subject to:

$$\text{Depth}(P_i) \geq 5 \tag{5}$$

$$P_i \text{ within } S_P \tag{6}$$

Where, P_i represents the i -th buoy station with longitude and latitude coordinates and P_j represents the j -th buoy station. $d_{i,j}$ is the Euclidean distance between the station P_i and the station P_j . $Nb(P_i)$ denotes the spatial neighborhood of P_i . The equation (3) indicates to get the minimum of $d_{i,j}$. For i and j which are from 1 to n , if P_j in the spatial neighborhood of P_i , $d_{i,j}$ is calculated, otherwise, $d_{i,j}$ is not calculated. STD is the operational function of standard deviation. S_{vj} is the area of EMR of P_j which is in $Nb(P_i)$. $\text{Depth}(P_i)$ denotes the water depth in the position of P_i . S_P denotes a specific solution space in the form of polygon geometry.

In the MOLMofOBS above, two key elements need to be calculated, namely, EMR and $Nb(P_i)$. In practice, the buoy monitoring stations are distributed discretely on the sea. A set of isolated coordinate points cannot intuitively express the spatial proximity between monitoring stations, nor can it record the adjacent stations of each monitoring station in a quantitative way. Actually, in addition, the boundary of each EMR cannot be delineated effectively. To estimate EMR and $Nb(P_i)$, a spatial neighborhood model is built in the next section.

3.2 Building the spatial neighborhood model of ocean moored buoys stations

In this section, a spatial neighborhood model (SNM) is established to represent the neighborhood and delimit the EMR of each station, shown in Figure 1. Firstly, the concept of a Voronoi diagram (Dong, 2008; Okabe et al., 2008; Lee, 2010) is employed to

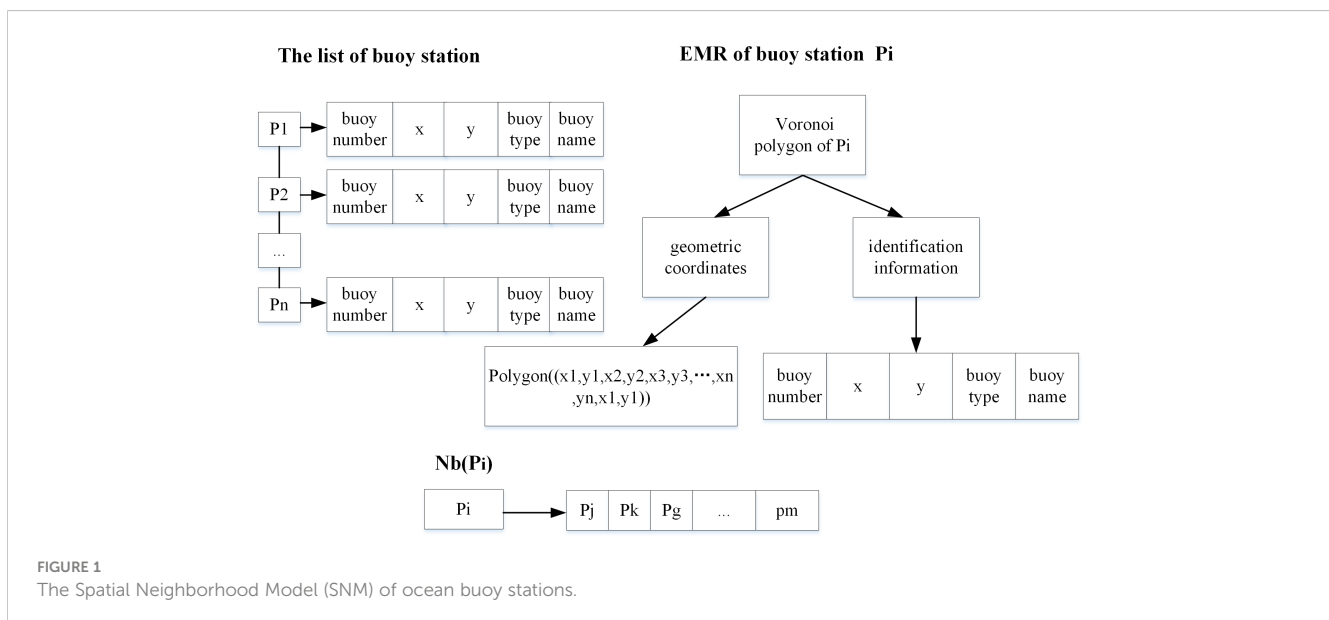


FIGURE 1 The Spatial Neighborhood Model (SNM) of ocean buoy stations.

divide the sea space; all buoy stations are treated as parent points to generate a Voronoi diagram, and each buoy station belongs to a Voronoi polygon. Inevitably, each Voronoi polygon is adjacent to other Voronoi polygons. If there is a common edge between the Voronoi polygon of station P_i and the Voronoi polygon of station P_j , P_i and P_j are adjacent. This kind of adjacent relationship is named the first-order Voronoi vicinity (1-oVv), which is adopted to measure the spatial proximity of ocean buoy stations and eliminate the effect of space barriers caused by linear obstacles, such as peninsulas or islands. $Nb(P_i)$ denotes the 1-oVv neighborhood (1-oVvN) of station P_i . A well-defined SNM is formed, as shown in Figure 1, with three components including a list of buoy stations, the EMR, and the 1-oVvN of every buoy station. The list of buoy stations includes their longitude, latitude, and identification information, such as buoy name, buoy number, and buoy type, which are the original data for location computation. Voronoi divides the entire study space and the distance between each point in the Voronoi polygon and its internal buoy station is closer than that between it and other buoy stations. Using Voronoi polygons to estimate the EMR can not only ensure that the spatial coverage of the buoy monitoring station is continuous in the whole study area, but also meet the requirement of spatial proximity. Therefore, the EMR of each buoy station is delimited by its Voronoi polygon.

4 A customized heuristic approach based on the MOPSO algorithm to solve MOLMofOBS

The MOLMofOBS in Section 3.1 is a typical multi-objective optimization problem. A heuristic method based on the MOPSO algorithm is designed to calculate near-optimization solutions of MOLMofOBS by expanding the advantages of simulating the social behavior of the population with the intelligence of the colony, sharing information among individuals, and working collaboratively. In the proposed MOPSO-based algorithm, the particle is a basic unit to calculate F1 and F2 defined in equations (3) and (4). It has two attributes of the position and the flight velocity. The position of a particle is a coordinate sequence of all buoy positions to be deployed. It is represented as $(x_1, y_1, x_2, y_2, x_3, y_3, \dots, x_n, y_n)$, where a pair of (x, y) stands for the position coordinate of a buoy station. So, a particle position contains positions of all buoys. The flight velocity of a particle is a sequence of all changes in the position of buoys and represented as $(v_1^x, v_1^y, v_2^x, v_2^y, v_3^x, v_3^y, \dots, v_n^x, v_n^y)$. Each component of the particle's velocity is added to the corresponding component of its position to obtain a new position of the particle. The new position of a particle will be divided into the coordinates of n buoy stations to calculate F1 and F2. A swarm of particles work to get new positions like above simultaneously.

The proposed MOPSO-based algorithm has a strong advantage in solving the problem of multi-station site selection because the position and flight velocity dimensions of each particle only need to be expanded horizontally, as the number of stations to be calculated

increases without enlarging the computational complexity. Compared to the traditional MOPSO algorithm, the improvement of the proposed MOPSO algorithm includes extending the formulas of adjusting particles' position and velocity to support multiple buoy stations and creating a strategy of adaptively tuning IW to diversify the particle individuals.

4.1 Adjustment formulas of particles position and velocity to support multiple buoy stations

Extending the adjustment formulas of particles position and velocity to accommodate multiple buoy stations is the crucial step for solving the MOLMofOBS in the MOPSO heuristics framework. Commonly, the population of particles move in a two-dimensional feasible solution space, and each individual particle is supposed to be a potential optimal solution. As the coordinate of each buoy station is composed of a longitude as the x -axis and a latitude as the y -axis, in the case of the n ($n \geq 1$) buoy stations location problem, the position of the i th particle containing coordinates of n buoy stations is extended to a $2 \times n$ -dimensional vector which is denoted using formulas (7):

$$(x_{i,1}(t), y_{i,1}(t), x_{i,2}(t), y_{i,2}(t), \dots, x_{i,n}(t), y_{i,n}(t)) \quad (7)$$

Similarly, the i th particle velocity vector is expressed using formulas (8):

$$(v_{i,1}^x(t), v_{i,1}^y(t), v_{i,2}^x(t), v_{i,2}^y(t), \dots, v_{i,n}^x(t), v_{i,n}^y(t)) \quad (8)$$

According to the principles of basic particle swarm optimization, the formulas (9) and (10) are designed to update the position and velocity of the particle in the x component, and the formulas (11) and (12) are used to update the position and velocity of the particle in the y component.

$$v_{ij}^x(t+1) = \omega v_{ij}^x(t) + c_1 r_1 (P_{ij}^x - x_{ij}(t)) + c_2 r_2 (P_{gj}^x(t) - x_{ij}(t)) \quad (9)$$

$$x_{ij}(t+1) = x_{ij}(t) + v_{ij}^x(t+1) \quad (10)$$

$$v_{ij}^y(t+1) = \omega v_{ij}^y(t) + c_1 r_1 (P_{ij}^y - x_{ij}(t)) + c_2 r_2 (P_{gj}^y(t) - x_{ij}(t)) \quad (11)$$

$$y_{ij}(t+1) = y_{ij}(t) + v_{ij}^y(t+1) \quad (12)$$

In which, ω is the inertia weight factor (IW) which is varying between 0 and 1. c_1 and c_2 are the acceleration coefficients, usually $c_1 = c_2 = 2$. r_1 and r_2 are random numbers varying between 0 and 1. t is the current iteration number. The position of buoy j is expressed in the reference frame located at particle i . The index j used for buoys extends from $j=1$ to n and the index i used for particles extends from $i=1$ to m . n is the number of buoy stations and m is the number of particles. $X_{i,j}(t)$ is the x component of the coordinate of the buoy station j reflected in the position of the particle i in the t th iteration. $v_{ij}^x(t+1)$ is the velocity of x_{ij} in the $(t+1)$ th iteration. P_{ij}^x is the x component of the individual best solution of the particle i for the buoy station j . P_{gj}^x is the x component of the global best

solution of the buoy station j . $y_{i,j}(t)$ is the y component of the position coordinate of the buoy station j embodied in the position of the particle i in the t th iteration. $v_{i,j}^y(t+1)$ is the velocity of $y_{i,j}$ the $(t+1)$ th iteration. $P_{i,j}^y$ is the y component of the individual best solution of the particle i for the buoy station j . P_{gi}^y is the y component of the global best solution of the buoy station j .

Formulas (7) to (12) in this part have been partially used in the paper wrote by song et al (Song et al., 2021), but without these necessary formulas, this paper would be difficult to understand. Therefore, in order to make this paper more readable and convenient for readers, these formulas are listed and illustrated here again.

4.2 Design of a dynamic inertia weight strategy

A dynamic inertia weight strategy (DIWS) is designed to adapt spatial proximity and improve the convergence and solution accuracy of optimization. The proposed DIWS focuses on adaptively adjusting the value of IW (ω) according to the variation rate of the objective values to eliminate the potential iteration stagnation brought by velocity linear attenuation and increase the diversity of particles searching behavior. The specific working mechanism of the DIWS is detailed as follows: on the one hand, when the variation rate of objective values is high, the IW is decreased to make the search step of the particles smaller so that they fly at a lower velocity. As the particles fly at a lower velocity, the number of particles in sparse regions will be increased to make the distribution of particles denser. So, a smaller IW can intensify a local search. On the other hand, when the variation rate of objective values is low, the IW is increased to make the flight step of the particles larger so that they fly at a higher velocity. As the particles fly at a higher speed, it is much more possible for them to jump out of the local search area and avoid search stagnation, so as to find new near-optimal solutions. So, a larger IW can promote a global search.

To realize the above principles, while comprehensively analyzing the characteristics of the variation rate of objective values, and comparing the variation characteristics of the classical mathematical functions (e.g., exponential, logarithmic, and power functions), we propose an empirical formula to adjust the value of IW based on the exponential function of the natural constant (e). The formula is shown as follows:

$$\omega_j^{t+1} = \begin{cases} e^{\partial-1}, & 0 < \partial < 1 \\ e^{(1/\partial)-1}, & \partial \geq 1 \end{cases} \quad (13)$$

$$\partial = \frac{rate_i^t}{rate_i^{t-1}} \quad (14)$$

$$rate_i^t = \quad (15)$$

$$0.367 \leq \omega^{t+1} \leq 1 \quad (14)$$

where ω_j^{t+1} is the IW factor of particle j in the $(t+1)$ th run; e is the natural constant; t is the current iteration number; k is the number of the objective functions; $f_i((x_1^j, y_1^j, \dots)^t)$ is the value of the objective function f_i of particle j in the t th iteration; $rate_i^t$ is the difference of all objective function values between two adjacent iterations; w_i is the preference weight, which is used to adjust different objective values to make their magnitude the same; and ∂ is the variation rate of the objective values. The variation curve of the IW value with the change rate of the objective values is shown in Figure 2.

4.3 The workflow to solve the multi-objective location problem of ocean buoy station using the MOPSO algorithm with DIWS

A workflow using the MOPSO algorithm with DIWS, named DIWS-MOPSO, is designed in a heuristic framework to ensure the MOLMoF OBS can be solved more efficiently and reliably. The workflow is illustrated in Figure 3 and the detailed steps are described as follows.

Step 1. Prepare spatial data.

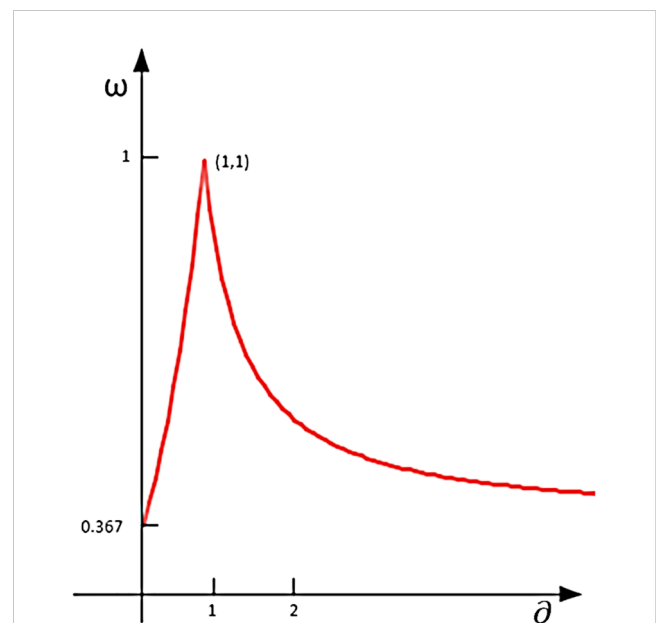
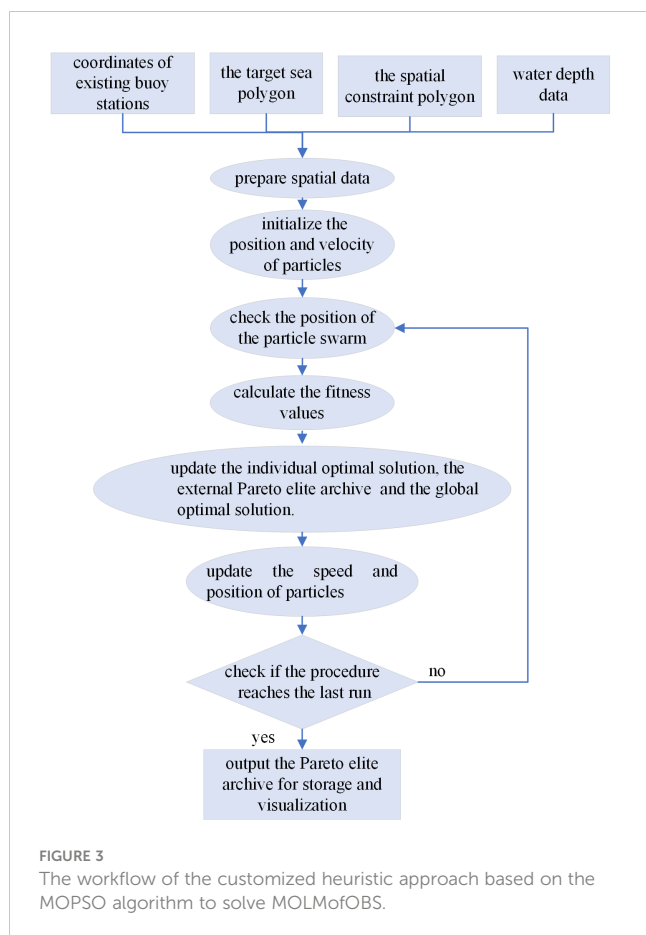


FIGURE 2 Variation curve of the inertia weight factor (ω) according to the change rate of the objective values (∂). It can be observed from Figure 2 that ω_j^{t+1} increases with the increase of ∂ . When $0 \leq \partial < 1$. The large ∂ indicates that the objective values calculated by two adjacent iterations are close, and the diversity of particles is decreased. Increasing ω expands the local search to a much broader space. When ∂ approaches 0, ω is near 0.367. When $\partial \geq 1$, ω decreases with the increase of ∂ . A bigger ∂ indicates a bigger difference between the objective values calculated by two adjacent iterations. Decreasing ω increases the search intensity of particles. When ∂ approaches either 0 and infinity, ω is near 0.367. Therefore, in theory, such a DIWS has the potential to increase the diversity of particles and avoid local convergence.



The spatial data required for the multi-objective location calculation of ocean buoy stations described in this paper includes the following:

- A list of existing buoy stations, in the format of point geometry.

- A target sea polygon, denoted as $S_Polygon_1$, providing basic marine geographic information such as coastline, peninsula, islands, and isobar of 100 meters depth.

- A spatial constraint polygon, denoted as $S_Polygon_2$, taken as the feasible solution space to limit the position of particles to prevent them from crossing the boundary.

- ETOPO1 water depth data (Amante and Eakins, 2009) with a spatial resolution of 1 arc minute, used to provide the water depth of any point in the feasible solution space.

Step 2. Initialize the position and velocity of particles.

Firstly, the minimum velocity and the maximum velocity are set as -0.05 and 0.05. For each particle, the absolute value of the difference between the maximum velocity and the minimum velocity is multiplied by a random number between 0 and 1, and added to the minimum speed to produce a final computational result, which is set as the initial velocity of a particle. Then, the positions of all individuals are initialized in the particle swarm by utilizing the center point of $S_Polygon_2$ as the reference point to radiate around at random distances that are not out of $S_Polygon_2$. Finally, the initial value of IW is set as 1.

Step 3. Check the position of the particle swarm.

For each particle, we check whether the position of each point is outside of $S_Polygon_2$. If it is, it is moved to a position with specific offsets of the center point on both the x - and y -axes, where the x or y offset is set to $2/5$ of the x or y distance between the point that is on the boundary of $S_Polygon_2$ and closest to the out-of-boundary point in the particle's position, and the center point of $S_Polygon_2$. If the water depth at the station point is less than 5 meters, a point with a water depth of more than 5 meters and 1 nautical mile away will be searched as a substitute.

Step 4. Calculate the fitness values.

For each particle, the coordinates of n buoy sites are parsed from the position vector of each particle and combined with the existing buoy sites to form a complete set of buoy sites. A Voronoi diagram of all buoy stations is generated by the algorithms described in Section 3.2, and the 1-oVvN of each station is calculated. For all station sites with a 1-oVv neighborhood relationship, the fitness values are calculated using equations (3) and (4). The calculated fitness value is a two-tuple group, denoted as (f_1, f_2) .

Step 5. Update the individual optimal solution.

For each particle, according to the Pareto dominance concepts, we update its individual optimal solution as follows. If f_1 and f_2 in the new solution are both superior to those in the old solution, that is, the new solution dominates the old solution, the new solution is set as the individual optimal solution. If the new solution is dominated by the old one, the new solution is discarded. If there is no dominant relationship between the new solution and the old one, then any solution is randomly selected as the individual optimal solution.

Step 6. Update the external Pareto elite archive.

An external elite archive is established to store Pareto non-inferior solutions. The external Pareto elite archive is updated as follows: first, the Pareto boundary of the current particle swarm is calculated, and the Pareto boundary and its corresponding particles are added to the elite archives. Second, an additional filter in the elite archive is applied according to the dominant relationship to remove all the dominated particles. Third, we determine whether the elite archive set exceeds the specified size. If it does, we use the crowding measurement method (Moubayed et al., 2014) to remove those particles with low crowding distance.

Step 7. Update the global optimal solution.

According to the crowding distance method, the particle and its fitness with the lowest crowding density is selected as the global best solution.

Step 8. Update the speed and position of particles.

For each particle, if the current run number is more than 4, the dynamic IW is calculated according to the formulas in Section 4.2. Otherwise, the IW value is fixed. The formulas in Section 4.1 are used to update the position and velocity before running to the next iteration.

Step 9. Check if the procedure reaches the last run.

If the last run has been reached, the algorithm outputs the Pareto elite archive for storage and visualization, and the iteration is quit. Otherwise, the algorithm goes to the step 3.

The differences between the calculation process in the DIWS-MOPSO heuristic framework and the traditional MOPSO include

the following: a) In step 2, the particle swarm initialization assignment method with the spatial center point as the reference point is used. b) Polygon geometric elements consisting of coastlines, isobaths, and islands are used as feasible solution spaces to constrain particles to prevent them crossing the spatial boundary in step 3. c) The IW is dynamically calculated in Step 10. All these measures effectively ensure that the proposed heuristic framework has good convergence, and that the obtained non-inferior solutions have good accuracy.

5 Experiments

A series of experiments is conducted to verify the effectiveness of the MOLMofOBS and the performance of the DIWS-MOPSO. Meanwhile, the convergence of the algorithm and the diversity of the non-inferior solutions are compared. Bohai Bay of China is selected as the study area, and the region delineated by the red polygon in Figure 4 is set as the feasible solution space. Although the two objectives F1 and F2 belong to different dimensions, they are compared separately without cross comparison, so no normalization processing is needed in the following experiments.

5.1 Performance analysis of DIWS-MOPSO for single buoy station location problem

In this section, a set of experiments is conducted by computing the single buoy station location problem using both the MOPSO algorithm with the fixed IW (IW-MOPSO) and the DIWS-MOPSO algorithm to prove the correctness and efficiency of these two heuristic algorithms and compare their performance. The performance evaluation indexes adopted in this paper include the following:

(1) Convergence evaluation index

Generation Distance (GD) (Menchaca-Mendez and Coello, 2015), representing the distance between the obtained Pareto

non-inferior solutions and the real Pareto frontier, is used to measure convergence, where a smaller GD value indicates that the calculation result is closer to the real Pareto frontier. The formula used to calculate GD value is as follows:

$$GD = \frac{1}{n} \left(\sum_{i=1}^n d_i^p \right)^{1/p}, \quad (16)$$

where n is the number of Pareto non-inferior solutions, p is the number of objectives, and d_i is the Euclidean distance between the i th Pareto non-inferior solution and the nearest solution of the real Pareto frontier in the objective space.

(2) Distribution uniformity evaluation index

The distribution uniformity of Pareto non-inferior solutions on the real Pareto frontier is measured by space metric (SD), where a smaller SD indicates a more uniform distribution of Pareto non-inferior solutions. The formula used to calculate SD is as follows:

$$SD = \sqrt{\frac{1}{n-1} \sum_i (\bar{d} - d_i)^2} \quad (17)$$

where $d_i = \min(|f_1^i(x) - f_1^j(x)| + |f_2^i(x) - f_2^j(x)|)$ ($i, j=1,2,\dots, n, i \neq j$). n is the number of Pareto non-inferior solutions; and \bar{d} is the mean of d_i .

In these experiments, the particle size is set to 100, the archive set size is set to 200, the initial search step is 0.05, and the number of iterations varies in terms of 100, 200, 400, 600, 800, and 1000. Experiment results are shown in Figures 5–7. Figure 5 shows a comparison of the real Pareto frontier obtained and Pareto non-inferior solutions calculated by IW-MOPSO and DIWS-MOPSO with 1000 iterations. It can be observed from Figure 5 that most of the Pareto non-inferior solutions (green triangles in Figure 5) obtained by both IW-MOPSO and DIWS-MOPSO are within the objective space formed by the real Pareto frontier (red diamonds in Figure 5), which indicates that the Pareto non-inferior solutions are all efficient solutions. In another aspect, the principal space of solutions obtained by IW-MOPSO is [16694, 52525] in the F1 term and [8.39E+09, 9.02E+09] in the F2 term, as shown in the lower-left area of Figure 5A, and the principal space of solutions obtained by DIWS-MOPSO is [13863, 54909] for F1 and [8.37E+09, 9.12E+09] for F2, as shown in the lower-left area of Figure 5B. These results indicate that the solutions space of DIWS-MOPSO is much wider than that of IW-MOPSO, which means the evolution of particle swarm in the DIWS-MOPSO algorithm is more diverse than that in the IW-MOPSO algorithm.

Figure 6 shows a convergence comparison between IW-MOPSO and DIWS-MOPSO using GD values, where the GD value of the DIWS-MOPSO algorithm is smaller than that of IW-MOPSO for each group of data with the same number of iterations. Furthermore, as the number of iterations increases, the GD value of IW-MOPSO fluctuates greatly. However, with the increase of the number of iterations, the GD value of DIWS-MOPSO gradually decreases, showing a stable trend on the 200th iteration, and finally becomes stable between 2.6E+06 and 3.2E+06. These results indicate that the stability of the DIWS-MOPSO algorithm is better, and the corresponding solutions are more concentrated. On the other hand, it can be observed from Figure 7 that the SD value of DIWS-MOPSO is smaller than that of IW-MOPSO as the

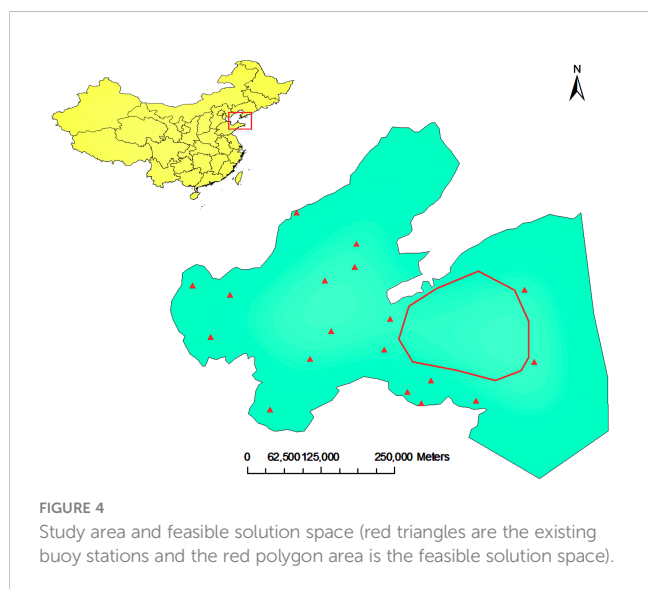


FIGURE 4 Study area and feasible solution space (red triangles are the existing buoy stations and the red polygon area is the feasible solution space).

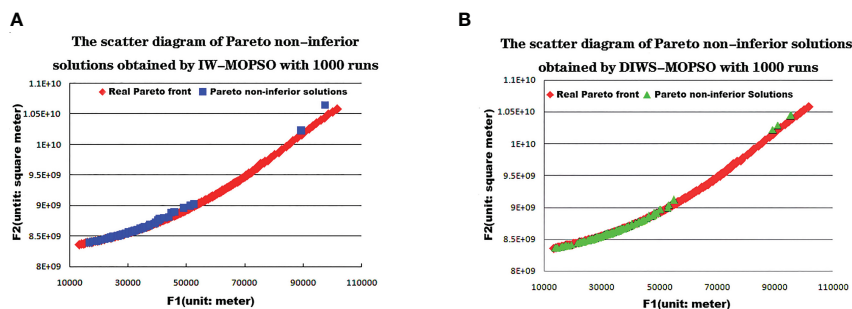


FIGURE 5 The scatter diagrams of Pareto non-inferior solutions obtained by IW-MOPSO and DIWS-MOPSO with 1000 runs for single buoy station location selection. (A) Pareto non-inferior solutions of IW-MOPSO (B) Pareto non-inferior solutions of DIWS-MOPSO.

number of iterations varies. Therefore, the distribution of Pareto non-inferior solutions obtained by DIWS-MOPSO is more uniform in the objectives space than that obtained by IW-MOPSO.

Based on the above results, MOPSO-based heuristic algorithms are effective in solving the single buoy station location problem, and the obtained Pareto non-inferior solutions can approximate the real Pareto frontier. Furthermore, the proposed DIWS-MOPSO algorithm has better stability and convergence than the IW-MOPSO algorithm, and the non-inferior solutions obtained by DIWS-MOPSO are more diverse and more evenly distributed than that obtained by IW-MOPSO in objective spaces.

5.2 Experiments solving multiple buoy stations location problem

Experiments are conducted on the location problem for 2, 3, 4, 5, and 6 buoy stations. To more closely observe the convergence effect of the algorithms, the particle size is set to 10, the number of iterations is set to 10, 20, 40, 60, 80, 100, 200, 400, or 600, the initial search step (i.e., particle velocity) is set to 0.05 arc-degrees, and the speed range is $[-0.05, 0.05]$. In fact, it is impossible to calculate the real Pareto frontier of the multiple buoy station location problem in a limited time as it is an NP problem, and, as such, it can rarely determine the optimal GD values. Instead, the layout pattern, which

is referred to as a description of the spatial features distribution in terms of being random, clustered, and dispersed, is adopted to measure the convergence of the algorithms in the performance comparison. In our application, the pattern that is more dispersed, more uniform in spatial distribution, and more balanced in distance between buoy stations is considered to be an acceptable and good pattern, which is used as a standard to evaluate the advantages and disadvantages of the algorithm calculation results. Here, we visually judge the patterns qualitatively.

The results of the experiments are given in Table 1, including good patterns obtained by the IW-MOPSO algorithm and the DIWS-MOPSO algorithm as the number of buoy station changes and the number of iterations required to obtain an acceptable and good pattern. An acceptable and good pattern is a spatial layout in which the value of F1 is biggest and the value of F2 is as smallest in a specific scenarios of buoy deployments. It can be observed that as the number of buoy stations (denoted by n) increase, the number of iterations required to obtain a good pattern increases continuously. When $n=2$, only 10 iterations are needed to generate a good pattern. However, when $n=6$, several hundred iterations are needed for a good pattern. When $n \geq 4$, as the number of buoys increases, the number of iterations required for DIWS-MOPSO to converge to a good pattern becomes much less than that of IW-MOPSO. Moreover, the gap between these two algorithm also increases as n increases. For example, when $n=5$, the number of iterations differs by only 20 between the two methods, whereas when $n=6$, the IW-MOPSO method converges to a fine pattern after 600 iterations, but the DIWS-MOPSO method requires only 200 iterations (a difference of 400 iterations). The number of iterations represents the convergence of the algorithm, where the fewer the number of iterations, the faster the convergence. Therefore, it is proved by the above experiments that the convergence of the DIWS-MOPSO algorithm is better than that of the IW-MOPSO algorithm, and this advantage becomes more obvious as n increases in the situation of multiple buoy stations location selection. In addition, with the same number of iterations, the non-inferior solution set obtained by DIWS-MOPSO is more diverse than that of IW-MOPSO. Therefore, after involving the DIWS in the MOPSO algorithm, it becomes much easier to obtain the new Pareto non-inferior solutions, and the diversity of the particle swarm is greatly improved as well.

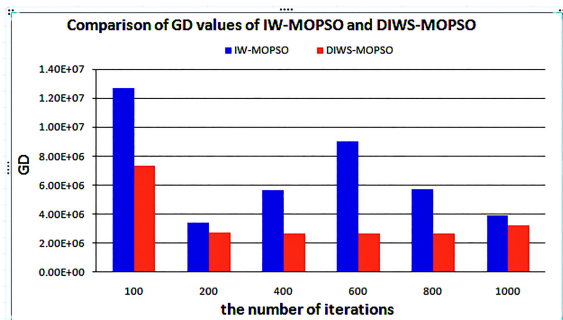
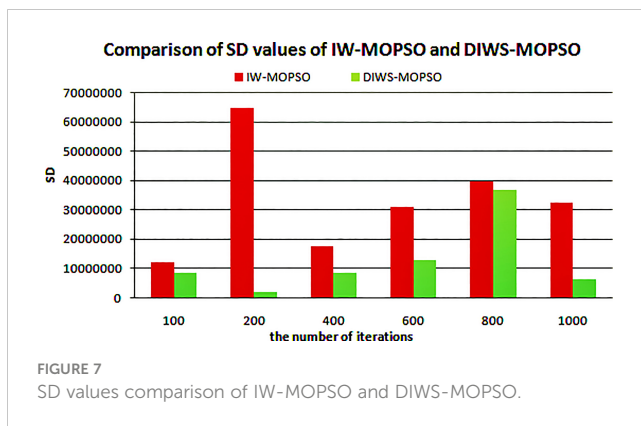


FIGURE 6 Convergence comparison of IW-MOPSO and DIWS-MOPSO algorithms by GD values.



From the experiments of the multi-buoy station location problem, we deduce that the optimal solution selection method based on the spatial pattern has important practical value. An MOPSO algorithm based on the swarm intelligence mechanism has the trait of searching for the extremum of the objective functions. However, if the extreme value of the objective function is pursued blindly, it is easy for the search to fall into the extreme region. For example, in the minimum value area of F2, the value of F1 is too large, and in the minimum value area of F1, the value of F2 is too large—both of which show solutions with a poor spatial pattern, which is reflected in the fact that some stations are far away from each other, and some stations are especially close and not scattered enough. In practice, neither of these results is what the decision-makers want. Therefore, the pattern-preferred approach provides an effective method for decision-makers to filter non-inferior solutions.

6 An ocean buoy location real-time planning portal

By integrating the ocean buoy location model, the SNM, and two kinds of MOPSO algorithms (i.e., IW-MOPSO and DIWS-MOPSO), an interactive portal is developed in the Cyberinfrastructure (CI) framework, which is a promise solution to enable spatial computing modules in web (Li et al., 2015; Miaomiao et al., 2016; Li et al., 2016a; Li et al., 2016b), to provide decision-making services for online ocean buoy station location real-time planning. The Architecture of the CI portal includes the data layer, the computing layer, and the presentation layer from bottom to top. The coordinates of buoy stations, electronic navigation charts and water depth data are stored using the PostgreSQL database in the data layer. The ocean buoy location model, the SNM, and the MOPSO-based algorithms including IW-MOPSO and DIWS-MOPSO are integrated in the computing layer using Python programming platform. Finally, the target sea area, Voronoi polygons and position points of buoy stations are visualized in the presentation layer using web programming technologies. This portal presents a unique Web-based spatial

analysis platform for buoy location selection, which is different from other existing portals.

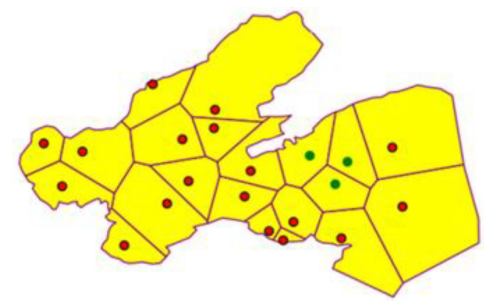
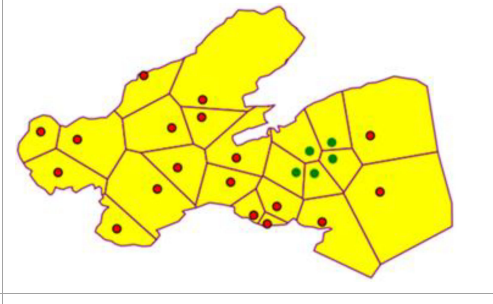
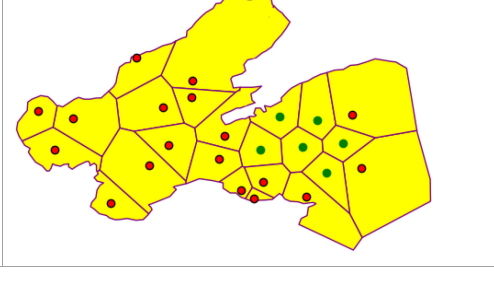
In the CI portal, the target sea area is selected by drawing a polygon on the online map, and the operation parameters (e.g., the particle size, buoy station count, the number of iterations, and the initial search step) can be tuned on demand and adjusted in real time. The arbitrary shape of the sea area is supported as the calculation area, and the calculation results are displayed in real time and are able to be operated interactively. Furthermore, both of the algorithms (IW-MOPSO and DIWS-MOPSO) are provided for online calculation, and the computational results can be compared visually for the selection of the optimal planning references. In addition, the portal also provides auxiliary tools for measuring distance and calculating area. Figure 7 shows the interface of the CI portal and demonstrates the calculation results of the three buoy stations. The red polygon is the target area drawn interactively, the small blue icons are the existing buoy stations, the green dots stand for the calculated buoy placement positions, and the blue lines are the boundaries of the Voronoi polygons. In Figure 8, four sets of calculation results were obtained and listed in the tree control on the left side of the interface. Ten particles were used to iterate 10 times and 100 times by the IW-MOPSO and DIWS-MOPSO algorithms, respectively. Each result set also contains several solutions, which can be visualized on the map to show a spatial pattern. Through this interactive and visualized portal, decision-makers can grasp the buoy distribution from a global perspective and select a layout scheme with a fine pattern according to actual needs.

7 Conclusion

This research reports the procedures and techniques for spatial optimization modeling of multi-objective locations of ocean buoy stations. Structuring the issue of ocean buoy station location selection as an explicit spatial optimization problem, as well as building an efficient heuristic algorithm to solve the problem and present computational results, effectively supports decision-making in ocean buoy observation network layout planning. In this paper, the MOLMofOBS is established by clear mathematical formulas based on Tobler's first law of geography. A Voronoi diagram is adopted to realize the spatial division of the target sea area for buoy observing, and an SNM is established to implement the spatial proximity estimation by measuring the 1-oVvN, ensuring the computability of the buoy station location model in practical applications. On the basis of sufficient investigation, comparative analysis, and testing, the traditional multi-objective PSO algorithm is improved by introducing a dynamic IW factor, and a new heuristic algorithm named DIWS-MOPSO is established.

In the DIWS-MOPSO algorithm, the dynamic formula of IW factor is designed, and the IW factor of each particle is calculated in real time according to the change rate of objective values in each run. The experimental results have proved that the DIWS-MOPSO algorithm has a great improvement in performance over IW-

TABLE 1 Comparison of selection results of multi-buoy stations location.

Number of buoy stations	IW-MOPSO		DIWS-MOPSO	
	a fine pattern	T ¹	a fine pattern	T ¹
2		10		10
3		20		20
4		60		20
5		80		60
6		600		200

1. T is the number of iterations required for a fine pattern.

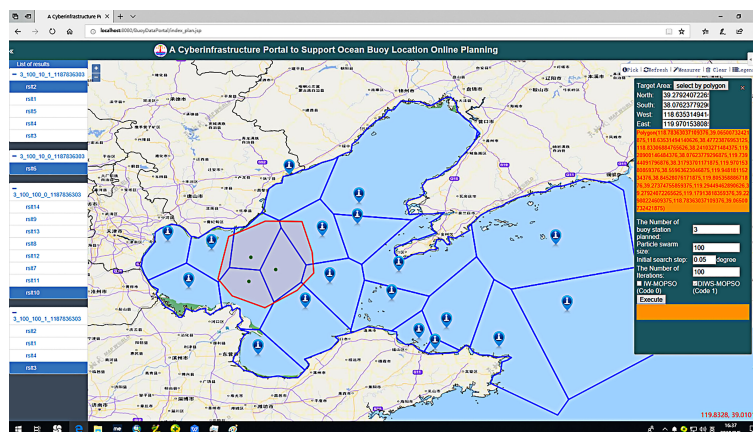


FIGURE 8

Screenshot of a cyberinfrastructure portal aggregating the SNM, the ocean buoy location model and the algorithms of IW-MOPSO and DIWS-MOPSO to support ocean buoy layout planning.

MOPSO. When calculating the buoy placement position, the DIWS-MOPSO algorithm not only effectively avoids local search stagnation, but also improves the diversity of non-inferior solutions. A spatial pattern is introduced to filter non-inferior solutions, and qualitatively judging the dispersion and aggregation of the ocean buoy layout pattern provides supplementary reference for decision-makers. Finally, we successfully integrated the proposed models and algorithms into an online analysis portal in the CI environment for real-time ocean buoy location planning. This portal provides a gateway and testbed where the general public, decision-makers, and researchers can select a target sea area by drawing a polygon directly on the map, change parameters on demand, and view computational buoy station locations immediately. To the best of our knowledge, this is the first time such spatial optimization modeling techniques have been developed and integrated into an interactive portal for ocean buoy location planning. This work has important significance for the sustainable development of marine buoy monitoring networks.

In the future, we will extend and deepen our research in the following aspects: first, we will further refine the site selection model. The influence of the spatial distribution of large-, medium-, and small-scale ocean phenomena such as water mass, cold/warm current, and ocean peak on the position of ocean buoy placement will be taken into account to restrict the spatial influence sphere of the buoy station in its corresponding Voronoi polygon, and a finer buoy spatial sphere model will be designed. Second, we will investigate the method of generating distance attenuation coefficients to calculate the effective monitoring coverage area of ocean buoy stations, aiming to accurately evaluate the ocean buoy monitoring density. Third, we will explore the potential of other heuristic algorithms (e.g., genetic algorithm, simulated annealing algorithm, and tabu algorithm) in solving the location problem of ocean buoy stations, as well as study the hybrid heuristic algorithm framework to improve the accuracy and spatial-temporal efficiency of calculation. Lastly, we will plan to promote the use of the multi-objective location modeling techniques of ocean buoy stations

planning in government departments and further improve it according to feedback provided. Spatial optimization modeling of multi-objective location of ocean buoy stations is a complex model, and will take much efforts for others to develop it to design buoy monitoring strategies. It's also our plan to open source the modeling code to benefit to the broad research communities and GeoAI (Hsu et al., 2021) technologies will be explored to speedup the computation of location selection of buoy deployments.

Data availability statement

The original contributions presented in the study are included in the article/Supplementary Material. Further inquiries can be directed to the corresponding authors.

Author contributions

SL and MS was responsible for the overall organization of the paper and wrote Section 1, Section 3, and Section 7. The contributions of SL and MS are equal and both the first author. MS and SC wrote Section 2. MS, XF, SZ, WH, SG, and KC wrote Section 4, Section 5, and Section 6. All authors contributed to the article and approved the submitted version.

Funding

This work is supported by the National Natural Science Foundation of China under Grant 41976179 and Grant 41801296; Strategic Research and Consulting Project of the Chinese Academy of Engineering (Grant No. 2022-XY-21); National Key Research and Development Program (2022YFC310203) and the Talent Training and Promotion Plan of Qilu University of Technology (Grant No. 2021PY06012).

Conflict of interest

The authors declare that the research was conducted in the absence of any commercial or financial relationships that could be construed as a potential conflict of interest.

Publisher's note

All claims expressed in this article are solely those of the authors and do not necessarily represent those of their affiliated

organizations, or those of the publisher, the editors and the reviewers. Any product that may be evaluated in this article, or claim that may be made by its manufacturer, is not guaranteed or endorsed by the publisher.

Supplementary material

The Supplementary Material for this article can be found online at: <https://www.frontiersin.org/articles/10.3389/fmars.2023.1134418/full#supplementary-material>

References

- AlvarezBenitez, J. E., Everson, R. M., and Fieldsend, J. E. (2005). *A MOPSO Algorithm Based Exclusively on Pareto Dominance Concepts[C]// Evolutionary Multi-Criterion Optimization, Third International Conference, EMO 2005* (Guanajuato, Mexico).
- Amante, C., and Eakins, B. W. (2009). *ETOPO1 1 arc-minute global relief model: Procedures, data sources and analysis* (Boulder, Colorado, USA: NOAA Technical Memorandum NESDIS NGDC-24).
- Amoshahy, M. J., Shamsi, M., and Sedaaghi, M. H. (2016). A novel flexible inertia weight particle swarm optimization algorithm. *PloS One* 11 (8), e0161558. doi: 10.1371/journal.pone.0161558
- Arana-Jiménez, M., Blanco, V., and Fernández, E. (2020). On the fuzzy maximal covering location problem. *Eur. J. Operational Res.* 283 (2), 692–705. doi: 10.1016/j.ejor.2019.11.036
- Atta, S., Mahapatra, P. R. S., and Mukhopadhyay, A. (2021). A multi-objective formulation of maximal covering location problem with customers' preferences: Exploring pareto optimality-based solutions. *Expert Syst. Appl.* 186, 115830. doi: 10.1016/j.eswa.2021.115830
- Blanco, V., and Gázquez, R. (2021). Continuous maximal covering location problems with interconnected facilities. *Comput. Operations Res.* 132, 105310. doi: 10.1016/j.cor.2021.105310
- Bourles, B., Lumpkin, R., Mchaden, M. J., Hernandez, F., Nobre, P., Campos, E., et al. (2008). The PIRATA program: History, accomplishments, and future directions. *Bull. Am. Meteorological Soc.* 89 (8), 435–447. doi: 10.1175/2008BAMS2462.1
- Casas-Ramírez, M.-S., Camacho-Vallejo, J., Díaz, J. A., and Luna, D. E. (2020). A bi-level maximal covering location problem. *Operational Res.* 20 (2), 827–855. doi: 10.1007/s12351-017-0357-y
- Chang, N. B., and Wei, Y. L. (2002). Comparative study between the heuristic algorithm and the optimization technique for vehicle routing and scheduling in a solid waste collection system. *Civil Eng. Syst.* 19 (1), 41–65. doi: 10.1080/10286600212162
- Chauhan, P., Deep, K., and Pant, M. (2013). Novel inertia weight strategies for particle swarm optimization. *Memetic Computing* 5 (3), 229–251. doi: 10.1007/s12293-013-0111-9
- Chen, G., Huang, X., Jia, J., and Min, Z. (2006). Natural exponential inertia weight strategy in particle swarm optimization. in *2006 6th World Congress on Intelligent Control and Automation, Dalian*. (Dalian, China: IEEE) pp. 3672–3675. doi: 10.1109/WCICA.2006.1713055
- Church, R. L., Stoms, D. M., and Davis, F. W. (1996). Reserve selection as a maximal covering location problem. *Biol. Conserv.* 76 (2), 105–112. doi: 10.1016/0006-3207(95)00102-6
- Church, R. L., and Wang, S. (2020). Solving the p-median problem on regular and lattice networks. *Comput. Operations Res.* 123, 105057. doi: 10.1016/j.cor.2020.105057
- Dong, P. (2008). Generating and updating multiplicatively weighted voronoi diagrams for point, line and polygon features in GIS. *Comput. Geosciences* 34 (4), 411–421. doi: 10.1016/j.cageo.2007.04.005
- Duque, J., Anselin, L., and Rey, S. J. (2012). The max-P-Regions problem. *J. Regional Sci.* 52 (3), 397–419. doi: 10.1111/j.1467-9787.2011.00743.x
- Feng, Y., and Liu, Y. (2013). A heuristic cellular automata approach for modelling urban land-use change based on simulated annealing. *Int. J. Geographical Inf. Sci.* 27 (3), 449–466. doi: 10.1080/13658816.2012.695377
- Feng, Y., Zheng, B., and Li, Z. (2010). Exploratory study of sorting particle swarm optimizer for multiobjective design optimization. *Math. Comput. Model.* 52 (11–12), 1966–1975. doi: 10.1016/j.mcm.2010.04.020
- Hase, H., Masumoto, Y., Kuroda, Y., and Mizuno, K. (2008). Semiannual variability in temperature and salinity observed by triangle trans-ocean buoy network (TRITON) buoys in the eastern tropical Indian ocean. *J. Geophysical Res. Oceans* 113 (C1), 1–10. doi: 10.1029/2006JC004026
- Hsu, C.-Y., Li, W., and Wang, S. (2021). Knowledge-driven GeoAI: Integrating spatial knowledge into multi-scale deep learning for Mars crater detection. *Remote Sens.* 13, 2116. doi: 10.3390/rs13112116
- Kashino, Y., Ueki, I., Kuroda, Y., and Purwandani, A. (2007). Ocean variability north of new Guinea derived from TRITON buoy data. *J. Oceanography* 63 (4), 545–559. doi: 10.1007/s10872-007-0049-y
- Kim, K., Dean, D. J., Kim, H., and Chun, Y. (2016). Spatial optimization for regionalization problems with spatial interaction: a heuristic approach. *Int. J. Geographical Inf. Sci.* 30 (3), 451–473. doi: 10.1080/13658816.2015.1031671
- Klippel, A., and Li, R. (2011). Interpreting spatial patterns: An inquiry into formal and cognitive aspects of tobler's first law of geography. *Ann. Assoc. Am. Geographers* 101 (5), 1011–1031. doi: 10.1080/00045608.2011.577364
- Knowles, J., and Corne, D. (1999). The pareto archived evolution strategy: A new baseline algorithm for pareto multiobjective optimisation. *Proc. Congress Evolutionary Computation*. doi: 10.1109/CEC.1999.781913
- Knowles, J. D., and Corne, D. W. (2014). Approximating the nondominated front using the pareto archived evolution strategy. *Evolutionary Comput.* 8 (2), 149–172. doi: 10.1162/106365605068167
- Kollat, J. B., and Reed, P. (2007). A framework for visually interactive decision-making and design using evolutionary multi-objective optimization (VIDEO). *Environ. Model. Software* 22 (12), 1691–1704. doi: 10.1016/j.envsoft.2007.02.001
- Köppen, M., and Veenhuis, C. (2006). Multi-objective particle swarm optimization by fuzzy-pareto-dominance meta-heuristic. *Int. J. Hybrid Intelligent Syst.* 3 (4), 179–186. doi: 10.3233/HIS-2006-3401
- Lee, I. (2010). Interactive analysis using voronoi diagrams: Algorithms to support dynamic update from a generic triangle-based data structure. *Trans. Gis* 6 (2), 89–114. doi: 10.1111/1467-9671.00099
- Li, W., Cao, K., and Church, R. L. (2016a). Cyberinfrastructure, GIS, and spatial optimization: opportunities and challenges. *Int. J. Geographical Inf. Sci.* 30 (3), 427–431. doi: 10.1080/13658816.2015.1112906
- Li, W., Church, R. L., and Goodchild, M. F. (2014). An extendable heuristic framework to solve the p-compact-regions problem for urban economic modeling. *Comput. Environ. Urban Syst.* 43 (1), 1–13. doi: 10.1016/j.compenvurbysys.2013.10.002
- Li, W., Song, M., Zhou, B., Cao, K., and Gao, S. (2015). Performance improvement techniques for geospatial web services in a cyberinfrastructure environment - a case study with a disaster management portal. *Computers Environ. Urban Syst.* 54, 314–325. doi: 10.1016/j.compenvurbysys.2015.04.003
- Li, W., Wu, S., Song, M., and Zhou, X. (2016b). A scalable cyberinfrastructure solution to support big data management and multivariate visualization of time-series sensor observation data. *Earth Sci. Inf.* 9 (4), 449–464. doi: 10.1007/s12145-016-0267-1
- Liu, Y., Yuan, M., He, J., and Liu, Y. (2015). Regional land-use allocation with a spatially explicit genetic algorithm. *Landscape Ecol.* 11 (1), 209–219. doi: 10.1007/s13555-014-0267-6
- Malcolma, S. A., and Revelle, C. (2005). Representational success: A new paradigm for achieving species protection by reserve site selection. *Environ. Modeling Assess.* 10 (4), 341–348. doi: 10.1007/s10666-005-9015-5
- Masoomi, Z., Mesgari, M. S., and Hamrah, M. (2013). Allocation of urban land uses by multi-objective particle swarm optimization algorithm. *Int. J. Geographical Inf. Sci. Ijgis* 27 (3), 542–566. doi: 10.1080/13658816.2012.698016
- McPhaden, M. J., Busalacchi, A. J., Cheney, R., Donguy, J.-R., Gage, K. S., Halpern, D., et al. (1998). The tropical ocean-global atmosphere observing system: A decade of progress. *J. Geophysical Res. Oceans* 103 (C7), 14169–14240. doi: 10.1029/97JC02906

- Menchaca-Mendez, A., and Coello, C. A. C. (2015). GDE-MOEA: a new MOEA based on the generational distance indicator and ϵ -dominance. *2015 IEEE Congress on Evolutionary Computation (CEC)*, 25–28 May 2015, Sendai, Japan. doi: 10.1109/CEC.2015.7256992
- Miaomiao, S., Song, M., Li, W., Zhou, B., and Lei, T. (2016). Spatiotemporal data representation and its effect on the performance of spatial analysis in a cyberinfrastructure environment - a case study with raster zonal analysis. *Comput. Geosciences* 87, 11–21. doi: 10.1016/j.cageo.2015.11.005
- Moubayed, N. A., Petrovski, A., and McCall, J. (2014). D2MOPSO: MOPSO based on decomposition and dominance with archiving using crowding distance in objective and solution spaces. *Evol. Comput.* 22 (1), 47–77. doi: 10.1162/EVCO_a_00104
- Murray, A. T. (2010). Advances in location modeling: GIS linkages and contributions. *J. Geographical Syst.* 12 (3), 335–354. doi: 10.1007/s10109-009-0105-9
- Nguyen, K. T., Nhan, T. H. N., Teh, W. C., and Hung, N. T. (2021). The connected p-median problem on complete multi-layered graphs. *Discrete Mathematics Algorithms Appl.* 14 (03), 2150118. doi: 10.1142/S1793830921501184
- Nittis, K., Zervakis, V., Papageorgiou, E., and Perivoliotis, L. (2002). Atmospheric and oceanic observations from the POSEIDON buoy network: Initial results. *J. Atmospheric Ocean Sci.* 8 (2–3), 137–149. doi: 10.1080/10236730290004076
- Nittis, K., Perivoliotis, L., Korres, G., Tziavos, C., and Thanos, I. (2006). Operational monitoring and forecasting for marine environmental applications in the Aegean Sea. *Environ. Model. Software* 21 (2), 243–257. doi: 10.1016/j.envsoft.2004.04.023
- Okabe, A., Satoh, T., Furuta, T., Suzuki, A., and Okano, K. (2008). Generalized network voronoi diagrams: Concepts, computational methods, and applications. *Int. J. Geographical Inf. Sci.* 22 (9), 965–994. doi: 10.1080/13658810701587891
- Raquel, C. R., and Naval, P. C. (2005). An effective use of crowding distance in multiobjective particle swarm optimization. *Genet. Evolutionary Comput. Conference*. doi: 10.1145/1068009.1068047
- Rouault, M., Servain, J., Reason, C. J. C., Bourlès, B., Rouault, M. J., Fauchereau, N., et al. (2009). Extension of PIRATA in the tropical south-East Atlantic: an initial one-year experiment. *South Afr. J. Mar. Sci.* 31 (1), 63–71. doi: 10.2989/AJMS.2009.31.1.5.776
- Santana, R. A., Pontes, M. R., and Bastosfilho, C. J. A. (2009). A Multiple Objective Particle Swarm Optimization Approach Using Crowding Distance and Roulette Wheel. In *2009 Ninth International Conference on Intelligent Systems Design & Applications*. 30 November 2009 - 02 December 2009, Pisa, Italy. doi: 10.1109/ISDA.2009.73
- Shifa, M. A., Ma, S., He, J., Liu, F., and Yu, Y. (2011). Land-use spatial optimization based on PSO algorithm. *Geo-spatial Inf. Sci.* 14 (1), 54–61. doi: 10.1007/s11806-011-0437-8
- Soltanpour, A., Baroughi, F., and Alizadeh, B. (2020). A hybrid algorithm for the uncertain inverse p-median location problem. *Facta Universitatis Ser. Mathematics Inf.* 35 (5), 1399–1416. doi: 10.22190/FUMI2005399S
- Song, M., Liu, S., Li, W., Chen, S., Li, W., Zhang, K., et al. (2021). A continuous space location model and a particle swarm optimization-based heuristic algorithm for maximizing the allocation of ocean-moored buoys. *IEEE Access* PP (99), 1–1. doi: 10.1109/ACCESS.2021.3060464
- Taiwo, O. J. (2021). Maximal covering location problem (MCLP) for the identification of potential optimal COVID-19 testing facility sites in Nigeria. *Afr. Geographical Rev.* 40 (4), 16. doi: 10.1080/19376812.2020.1838306
- Tang, W., Yueh, S. H., Fore, A. G., and Hayashi, A. (2015). Validation of aquarius sea surface salinity with in situ measurements from argo floats and moored buoys. *J. Geophysical Res. Oceans* 119 (9), 6171–6189. doi: 10.1002/2014JC010101
- Tobler, W. R. (1970). A computer movie simulating urban growth in the Detroit region. *Economic Geogr.* 46 (Supp 1), 234–240. doi: 10.2307/143141
- Tong, D., and Murray, A. T. (2012). Spatial optimization in geography. *Ann. Assoc. Am. Geographers* 102 (6), 1290–1309. doi: 10.1080/00045608.2012.685044
- Uma, S. M., Rajiv Gandhi, K., and Kirubakaran, E. (2012). A hybrid PSO with dynamic inertia weight and GA approach for discovering classification rule in data mining. *Int. J. Comput. Appl.* 40 (17), 32–37. doi: 10.5120/5074-7471
- Wang, J., Wang, Z., Wang, Y., Liu, S., and Li, Y. (2016). Current situation and trend of marine data buoy and monitoring network technology of China. *Acta Oceanologica Sin.* 35 (2), 1–10. doi: 10.1007/s13131-016-0815-z
- Wang, K., Chen, N., Tong, D., Wang, K., Wang, W., and Gong, J. (2016). Optimizing precipitation station location: a case study of the jinsha river basin. *Int. J. Geographical Inf. Sci.* 30 (6), 1207–1227. doi: 10.1080/13658816.2015.1119280
- Wang, K., Gong, Y., Peng, Y., Hu, C., and Cheng, N. (2020). An improved fusion crossover genetic algorithm for a time-weighted maximal covering location problem for sensor siting under satellite-borne monitoring. *Comput. Geosciences* 136 (Mar.), 104406.1–104406.13. doi: 10.1016/j.cageo.2020.104406
- Wang, C., and Zhang, Z. (2012). A maximum loss minimization model for portfolio selection based on the CVaR measurement. *Advanced Materials Res.* 524–527, 3828–3833. doi: 10.4028/www.scientific.net/AMR.524-527.3828
- Xie, X., and Xu, Y. W. (2017). *Multi-sensor image fusion algorithm based on multi-objective particle swarm optimization algorithm* (Society of Photo-optical Instrumentation Engineers). doi: 10.1117/12.2295802
- Yang, P., Xiao, Y., Zhang, Y., Zhou, S., Yang, Y., and Xu, Y. (2020). The continuous maximal covering location problem in large-scale natural disaster rescue scenes. *Comput. Ind. Eng.* 146, 106608. doi: 10.1016/j.cie.2020.106608
- Zaferanieh, M., Abareshi, M., and Fathali, J. (2022). The minimum information approach to the uncapacitated p-median facility location problem. *Transportation Lett.* 14 (3), 307–316. doi: 10.1080/19427867.2020.1864595
- Zhao, F., Zhang, Z., and Zou, J. (2012). A new algorithm using pareto archive evolution strategy to multi-objective optimization problem. *Advanced Sci. Lett.* 6 (1), 406–410. doi: 10.1166/asl.2012.2237